

EPR and ENDOR investigation of the $[F_{Li}]^0$ center in CaO

M. M. Abraham, Y. Chen, D. N. Olson,* V. M. Orera,† T. M. Wilson,‡ and R. F. Wood

Solid State Division, Oak Ridge National Laboratory, Oak Ridge, Tennessee 37830

(Received 28 August 1980)

A new paramagnetic color center, denoted by $[F_{Li}]^0$, is reported. It has been observed in single crystals of CaO grown with lithium impurities. The center consists of a single electron in a O^{2-} vacancy with a Li^+ ion replacing an adjacent Ca^{2+} ion, i.e., an F^+ center next to a lithium substitutional impurity. Therefore, this is the first paramagnetic electron-defect center possessing local electrical neutrality to be seen in the alkaline-earth oxides. EPR and ENDOR measurements at both X and K band yield the following spin-Hamiltonian parameters at 4.2 K: $g_{||} = 1.9993(2)$; $g_{\perp} = 2.0001(2)$; $A = \mp 9.01(1)$ MHz; $B = \mp 5.35(1)$ MHz; and $P \leq 0.005$ MHz. The hyperfine values are temperature dependent and are also reported for 77 and 150 K. The data suggest that there is an outward relaxation of the lithium ion and probably other ions in the lattice, but there is no electric-field gradient.

I. INTRODUCTION

Color centers have long been studied in alkali halides. More recently, these studies have been extended to the alkaline-earth oxides. In the alkali halides, an F center is a single electron trapped in an anion vacancy. Its counterparts in the alkaline-earth oxides are the F^+ and F centers where one or two electrons, respectively, are trapped at O^{2-} vacancies. Although color centers in the alkali halides are now quite well understood, the situation is less satisfactory for the alkaline-earth oxides. This is due to the comparative paucity of data and the additional complexity resulting from the double charge of the ions.

The evidence for both the F^+ and F centers comes from optical measurements while only the paramagnetic F^+ center can be studied using electron paramagnetic resonance (EPR) and electron-nuclear double resonance (ENDOR) spectroscopy. EPR measurements in MgO ,¹ CaO ,²⁻⁴ SrO ,^{3,5} and BaO (Refs. 3, 6, and 7) gave g values which are close to the free-electron value. Clearly resolved magnetic hyperfine structure from an interaction with nearby magnetic nuclei (^{25}Mg , ^{43}Ca , ^{87}Sr and both ^{135}Ba and ^{137}Ba) were also observed, verifying that the electron wave function extends well into the surrounding lattice of anions and cations. ENDOR measurements have supplied even more precise hyperfine constants. In MgO the interactions with ^{25}Mg neighbors^{8,9} and ^{17}O neighbors¹⁰ have been measured beyond the first-neighbor shells, while in SrO , only the interaction with the first-neighbor ^{87}Sr nuclei¹¹ has been reported.

Additional information about the electronic wave function can be obtained by replacing nuclei adjacent to the F center with impurity nuclei having nonzero spin. For the alkali halides, when one of the cations is replaced by a monovalent impurity, the electrically

neutral center is called an F_A center. For the alkaline-earth oxides, impurity cations can be either monovalent or divalent, and the anion vacancy can be occupied by one or two electrons. To avoid confusion, we shall use the notation $[F_A]^0$ for centers consisting of either one electron in an anion vacancy adjacent to a monovalent-cation impurity or of two electrons in an anion vacancy adjacent to a divalent-cation impurity. Both of these possibilities possess local electrical neutrality. On the other hand, a single electron in the anion vacancy and a divalent-cation impurity, requiring nonlocal charge compensation, would then be noted by $[F_A]^+$. According to this convention, it is the nonparamagnetic $[F_{Mg}]^0$ in CaO which has been studied using optical methods¹² and the paramagnetic $[F_{Mg}]^+$ in CaO which has been the subject of EPR and optical investigations.¹³⁻¹⁵ A new center, the $[F_{Li}]^0$ in CaO, is reported here. This center is of particular interest because it is both paramagnetic and neutral with respect to the lattice. Additionally, the lithium nucleus has a large magnetic moment facilitating both EPR and ENDOR measurements.

II. EXPERIMENTAL PROCEDURE

Crystals of CaO doped with lithium were grown by the arc-fusion method in a reducing atmosphere in order to create nonstoichiometry. The resulting melt contained clear and dark regions. Some of the clear regions contained F^+ centers, while only the dark portions had both F^+ and $[F_{Li}]^0$ centers. No irradiation process was required and the centers were stable at room temperature. EPR spectra were obtained using K -band (~ 24.3 GHz) and X -band (~ 9.28 GHz) superheterodyne spectrometers with rectangular TE_{102} mode cavities. EPR linewidths were approximately

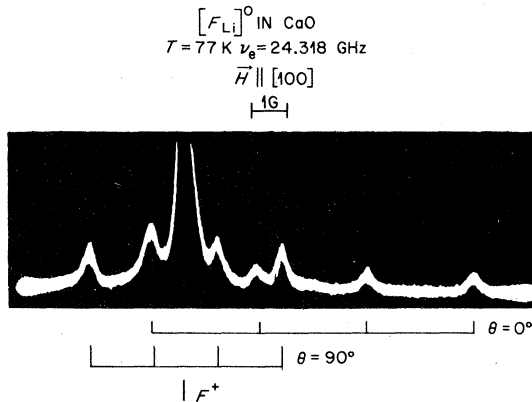


FIG. 1. EPR spectra of F^+ and $[F_{Li}]^0$ centers in CaO. The oscilloscope trace clearly shows two sets of four lines for the $[F_{Li}]^0$ center. One set, labeled $\theta = 0^\circ$, arises when the field is along the axis of the center, while for the other set labeled $\theta = 90^\circ$, the field is perpendicular to the axis. The isotropic F^+ center line is located at the center of the $\theta = 90^\circ$ set.

0.5 G full width at half maximum (FWHM). Magnetic fields were measured to within 0.1 G using a proton nuclear magnetic resonance (NMR) probe. The only other resonance signals of significance were due to Mn^{2+} impurities.

ENDOR transitions were induced by an rf field which was produced by a coil wound around the outside of the cavity. The field gained entry through a transverse slot cut in the end of the cavity, and the crystal was glued to the bottom of the cavity. The ENDOR linewidths were about 40 KHz full width at half maximum.

III. RESULTS AND DISCUSSION

An oscilloscope display of the EPR signal at K band with the magnetic field parallel to a crystal

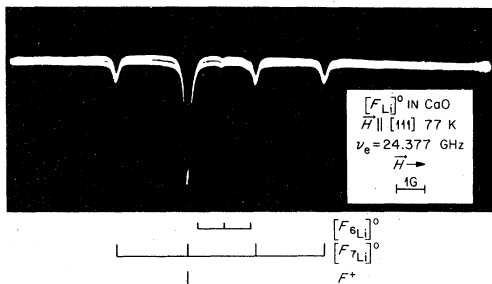


FIG. 2. EPR spectra of F^+ and $[F_{Li}]^0$ centers in CaO for the case where the magnetic field makes equal angles with the three orthogonal $[F_{Li}]^0$ center axes. This oscilloscope trace shows a small contribution from the 7% abundant ${}^6\text{Li}$ nuclei.

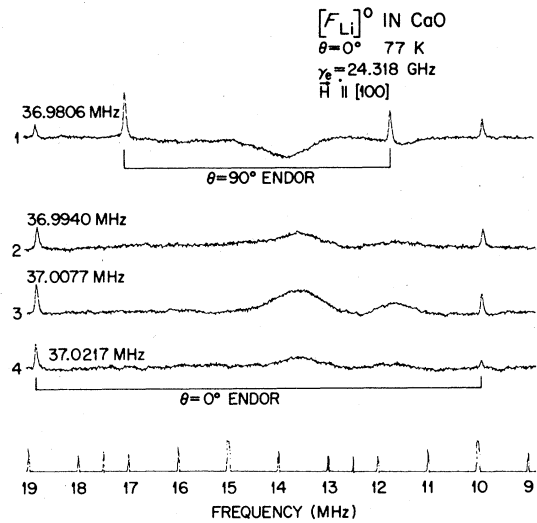


FIG. 3. ENDOR spectra of the $[F_{Li}]^0$ center in CaO with \vec{H} parallel to the defect axis. Individual traces were taken on different hyperfine lines labeled progressively from 1 (low field) to 4 (high field). Applied magnetic fields are specified in terms of proton nuclear resonance frequency.

$\langle 100 \rangle$ axis is shown in Fig. 1. Clearly visible is a large isotropic line and two sets of four lines. The former is due to the F^+ center and the latter are attributed to the $[F_{Li}]^0$ center, which is due to the interaction of an electron at an O^{2-} vacancy with a ${}^7\text{Li}^{+}$ ion ($I = \frac{3}{2}$) substituted for a Ca^{2+} ion in a nearest-

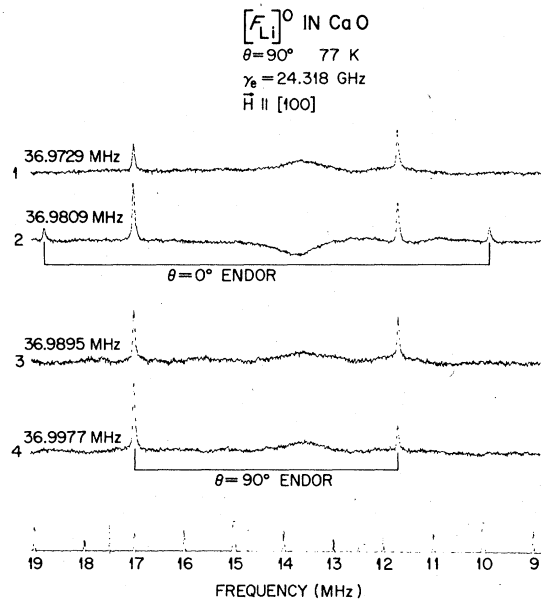


FIG. 4. ENDOR spectra of the $[F_{Li}]^0$ center in CaO with \vec{H} perpendicular to the defect axis. Individual traces were taken on different hyperfine lines labeled progressively from 1 (low field) to 4 (high field). Applied magnetic fields are specified in terms of proton nuclear resonance frequency.

neighbor site. The four-line set centered on the F^+ line, has twice the amplitude of the four-line set displaced to higher fields which suggests an axial symmetry site oriented along a $\langle 100 \rangle$ direction of the crystal and that g_{\perp} is the same as the isotropic g value of the F^+ center. This is further supported by the observed angular dependence, particularly the collapse to a single set of four lines along a $\langle 111 \rangle$ direction shown in Fig. 2. A three-line set due to the 7% abundant ^6Li nucleus ($I = 1$) is also visible in this orientation.

Each of the EPR transitions, saturated in turn, pro-

$$\mathcal{H} = \mu_B [g_{\parallel} H_z S_z + g_{\perp} (H_x S_x + H_y S_y)] + A I_z S_z + B (I_x S_x + I_y S_y) + P [I_z^2 - \frac{1}{3} (I + 1)] - g_N \mu_N \vec{H} \cdot \vec{I}, \quad (1)$$

where all the symbols have their usual significance. This expression has been used to fit the experimental data with the results shown in Table I. The fitting of the ENDOR signals gave a value for g_N of 2.170(1) which is within the experimental error for the published value for ^7Li . This confirms that the lithium dopant gives rise to the center. The difference of the nuclear magnetic moments for ^7Li and ^6Li accounts for the difference in the magnetic hyperfine splitting noted in Fig. 2.

The EPR spectrum obtained at X band produced different relative positions for the hyperfine lines compared to those obtained at K band. This difference was very helpful in confirming the assignment of the site. ENDOR measurements were also carried out at X band and, since the results agreed with the K -band data, the spin-Hamiltonian parameters shown in Table I are averages of both X - and K -band ENDOR measurements. An initial confusion about the hyperfine constants was resolved once it became clear that the temperature dependence was a real effect. This prompted us to look for additional verification by allowing the temperature to rise above 77 K. Using only the resonant frequency of the cavity as a guide to estimate the temperature, we obtained ENDOR signals at about 150 K which gave the values $A = \mp 8.86(3)$ MHz and $B = \mp 5.24(2)$ MHz.

TABLE I. Spin-Hamiltonian parameters for $[F_{Li}]^0$ centers.

| | | |
|-----------|-----------------------------|---------------|
| | $g_{\parallel} = 1.9993(2)$ | |
| | $g_{\perp} = 2.0001(2)$ | |
| 4.2 K | | 77 K |
| A (MHz) | $\mp 9.01(1)$ | $\mp 8.93(1)$ |
| B (MHz) | $\mp 5.37(1)$ | $\mp 5.30(1)$ |
| P (MHz) | < 0.005 | < 0.005 |

duced ENDOR signals. The ENDOR transitions are shown in Fig. 3 for sites aligned parallel to the magnetic field and in Fig. 4 for those aligned perpendicular to the magnetic field. The magnetic field for each transition is indicated at the left of each trace in terms of the NMR proton frequencies. Counting from the low-field line for the EPR transitions in Fig. 1, the second $\theta = 90^\circ$ line and the first $\theta = 0^\circ$ line can be seen to overlap. For this magnetic field, therefore, the ENDOR traces in Fig. 3 and 4 showed evidence of both transitions.

The spin Hamiltonian appropriate to this situation is

The alignment of the ENDOR transitions, one above the other, at the same rf frequency in Figs. 3 and 4 is an indication that the quadrupole splitting factor $P = 3e^2qQ/4I(2I - 1)$ is very small. We have placed an upper limit on P of 5 KHz based on the experimental linewidths.

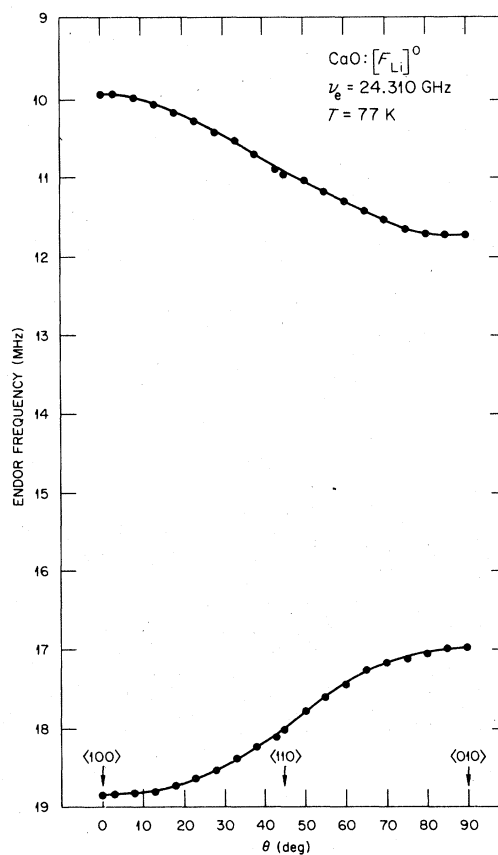


FIG. 5. Angular dependence of the ENDOR transitions for the $[F_{Li}]^0$ center in CaO. The absence of a line cross-over demonstrates that the hyperfine constants A and B have the same sign.

TABLE II. Decomposition of the magnetic hyperfine interaction.

| | a (MHz) | b (MHz) | $\langle R \rangle$ (Å) | $10^{-20} \psi(R_{Li}) ^2$ (cm ⁻³) |
|-------|--------------|--------------|----------------------------|--|
| 4.2 K | ∓ 6.583 | ∓ 1.213 | 2.94 | 255.8 |
| 77 K | ∓ 6.510 | ∓ 1.210 | 2.94 | 252.9 |

The sign of the magnetic hyperfine constants, A and B , must be the same since the angular dependence of the ENDOR transitions shown in Fig. 5 does not exhibit a crossover. Although the sign is not uniquely determined, point dipole considerations suggest that negative signs for A and B are the most likely (see below).

The magnetic hyperfine parameters from Table I can be decomposed into isotropic and anisotropic portions, $a = (A + 2B)/3$ and $b = (A - B)/3$. These are shown in Table II. The isotropic hyperfine constant a is related to the wave function ψ of the $[F_{Li}]^0$ electron at the ${}^7\text{Li}$ nucleus through the Fermi contact term

$$a = \frac{8\pi}{3h} \left(\frac{\mu_e}{S} \right) \left(\frac{\mu_N}{I} \right) |\psi(\bar{R}_{Li})|^2, \quad (2)$$

where \bar{R}_{Li} is the position of the Li ion with respect to the normal lattice site of the missing O^{2-} ion, at which the coordinate origin of $\psi(\bar{r})$ is chosen. The anisotropic hyperfine constant b in a point dipole approximation is given by

$$b = \frac{1}{h} \left(\frac{\mu_e}{S} \right) \left(\frac{\mu_N}{I} \right) \left(\frac{1}{\langle R^3 \rangle} \right), \quad (3)$$

where R is the effective electron-nuclear separation. According to the convention outlined by Abraham *et al.*¹⁶ where μ_e was considered positive for hole-type centers, μ_e will be considered as negative here. This leads to a negative sign for b and the signs of a , A , and B follow. The values for the derived quanti-

ties $\langle R \rangle$ and $|\psi(\bar{R}_{Li})|^2$ are also given in Table II.

The value of $\langle R \rangle$ is in surprisingly good agreement with the results of an elementary calculation. The normal lattice spacing in CaO is 2.40 Å and the F^+ center in the alkaline-earth oxides usually has about a 6–8% outward relaxation of the first-nearest-neighbor ions associated with it.^{8,17,18} Furthermore, the difference in radii between the Ca^{2+} and Li^+ ions is about 0.3 Å. Thus, if we assume that the Li^+ ion moves outward along the [100] direction to contact the negative ion at the (2,0,0) site (as it does in the $[F_{Li}]^0$ center in KCl),¹⁹ the distance between defect site (0,0,0) and the Li^+ ion becomes 2.90 Å (= 1.08 times 2.40 Å + 0.3 Å). If we further assume that the defect wave function is contained virtually entirely within a radius of 2.90 Å, the results for $\langle R \rangle$ in Table II are readily understood. Not only would $\langle R \rangle$ be expected to be ~ 2.94 Å but also $|\psi(\bar{R}_{Li})|^2$ would be small. The data in Table III, however, show clearly that the large value of $\langle R \rangle$ and small value of $|\psi(\bar{R}_{Li})|^2$ of the new $[F_{Li}]^0$ center are quite unusual when compared to the same quantities in other simple centers in the alkaline-earth oxides. The case of the $[F_{Mg}]^+$ center in CaO is particularly pertinent because the radii of the Li^+ and Mg^{2+} are almost identical and the same type and magnitude of lattice relaxation described above should hold for this center and the $[F_{Li}]^0$ center. It is therefore necessary to consider the differences between the two centers in more detail and this consideration leads very quickly to the conclusion that polarization of the wave function of the defect electron itself must be playing an important role in the $[F_{Li}]^0$ center.

TABLE III. Wave functions in the alkaline-earth oxides.

| | $10^{-20} \psi(R_v) ^2$ (cm ⁻³) | A_v | $10^{-20} \psi^0(R_v) ^2$ (cm ⁻³) | $\langle R \rangle$ (Å) | Ref. |
|---------------------|---|-------|---|----------------------------|-----------|
| $[F_{Li}]^0$ in CaO | 254 | 57 | 4.5 | 2.94 | This work |
| $[F_{Mg}]^+$ in CaO | 2034 | 325 | 6.3 | 1.87 | 15 |
| F^+ in MgO | 2722 | 325 | 8.4 | 1.54 | 8,9 |
| F^+ in CaO | 5760 | 700 | 8.2 | 1.25 | 4 |
| F^+ in SrO | 14210 | 1850 | 7.7 | 0.93 | 5,11 |
| F^+ in BaO | 28100 | 3300 | 8.5 | 0.76 | 7 |

The new center is electrically neutral on a scale of several lattice spacings, but on a more local scale it is not. The Li^+ ion has an effective negative charge in the CaO lattice and this charge will polarize the defect electron by introducing a Γ_4^- (p -type) component to the potential at the (0,0,0) site. The defect wave function can be written in the usual approximate form for this type of center as

$$\psi(\vec{r}) = N \left[\psi^0(\vec{r}) - \sum_{\nu,i} \langle \psi^0 | \phi_{\nu,i} \rangle \phi_{\nu,i}(\vec{r} - \vec{R}_\nu) \right] \quad (4)$$

in which $\psi^0(\vec{r})$ is the smooth part of the wave function, $\phi_{\nu,i}(\vec{r} - \vec{R}_\nu)$ is the i th core orbital on the ion at \vec{R}_ν , $\langle \psi^0 | \phi_{\nu,i} \rangle$ is the overlap integral between ψ^0 and $\phi_{\nu,i}$, and N is a normalization factor. In pure octahedral symmetry, $\psi^0(\vec{r})$ for the ground-state wave function is expected to be made up almost entirely of an s -type function (Γ_1^+) with perhaps a very small admixture of that combination of g -type components which transform as Γ_4^+ . The lowering of the O_h symmetry in the $[F_{Mg}]^+$ center in CaO may introduce a small component of p -type symmetry into ψ^0 but this admixture should be negligible in its effects on $\langle R \rangle$ and $|\psi(\vec{R}_{Mg})|^2$. In the $[F_{Li}]^0$ center, on the other hand, the effective negative charge at a nearest-neighbor site can be expected to introduce a large p -type admixture into ψ^0 . Unpublished calculations by two of the present authors (TMW and RFW) on V -type centers and on O^{2-} ions in alkaline-earth oxides with an effective unit charge at a first-neighbor site show that the admixture of a polarizing component into the wave function is of the order of 30–40%. Such an admixture will reduce ψ^0 in the vicinity of the Li ion and enhance it in the vicinity of the Ca^{2+} ion at the $(-1,0,0)$ position. We believe that this electronic polarization of the defect electron is the principal explanation of the large differences in the values of $\langle R \rangle$ for the $[F_{Li}]^0$ and $[Mg]^+$ centers.

Table III also shows values of the so-called amplification factor A_ν introduced by Gourary and Adrian²⁰ and values of $|\psi^0(R_\nu)|^2$ extracted by using this amplification factor. The value of A_ν for the Li^+ ion was taken from Ref. 20 and the values for the other positive ions in Table III were taken from Hughes and Henderson.²¹ If we assume that $\psi^0(\vec{r})$ is slowly varying in the regions of the $\phi_{\nu,i}$, the overlap integrals in Eq. (4) can be approximated by

$$\begin{aligned} \langle \psi^0 | \phi_{\nu,i} \rangle &\equiv \int \psi^0(\vec{r}) \phi_{\nu,i}(\vec{r} - \vec{R}_\nu) d\tau \\ &\approx \psi^0(\vec{R}_\nu) \int \phi_{\nu,i}(\vec{r} - \vec{R}_\nu) d\tau \end{aligned} \quad (5)$$

with the result that

$$\begin{aligned} \psi(\vec{r}) &\approx N \left[\psi^0(\vec{r}) - \sum_{\nu} \psi^0(\vec{R}_\nu) \sum_i \phi_{\nu,i}(\vec{r} - \vec{R}_\nu) \right. \\ &\quad \left. \times \int \phi_{\nu,i}(\vec{r}' - \vec{R}_\nu) d\tau' \right] \end{aligned} \quad (6)$$

Moreover, if the overlap integrals are small, $N \approx 1$ and the amplification factor for the ν th ion becomes

$$A_\nu = \left[1 - \sum_i \phi_{\nu,i}(0) \int \phi_{\nu,i}(\vec{r} - \vec{R}_\nu) d\tau \right]^2 \quad (7)$$

Here, the sum over i includes only s orbitals which are the only core orbitals that give nonvanishing spin densities at the nuclei. This factor is a property entirely of the core electrons²² and is tabulated in Table III for Li^+ , Mg^{2+} , etc., ions. It should be noted that the A_ν for the Li^+ and Mg^{2+} ions differ by a factor of approximately 6. This is primarily due to the double charge of the Mg^{2+} ion which causes the value of $\phi_{\nu,i}(0)$ for the $1s$ electrons to be much larger in Mg^{2+} than in Li^+ . The value of $|\psi^0(R_\nu)|^2$ at the Li^+ ion in the $[F_{Li}]^0$ center is significantly lower than it is at the Mg^{2+} ion in the $[F_{Mg}]^+$ center and this we also attribute to the polarization of the smooth part of the wave function in the former case.

It should be realized that Eq. (4) is itself an approximation and that the amplification factor A_ν is derived by further approximations to Eq. (4). Clearly, a more rigorous approach such as that taken in the calculations of Wood²³ and Harker²⁴ for the F center in the alkali halides are needed. These, however, must be preceded by reliable calculations of the electronic structure and lattice relaxation of this newly observed defect. Such calculations might also suggest why the quadrupole term is so small and why the temperature dependence of the hyperfine interaction is more pronounced in this center than in other somewhat similar centers.

ACKNOWLEDGMENT

Research sponsored by the Division of Materials Sciences, U.S. Department of Energy under Contract No. W-7405-eng-26 for the Union Carbide Corporation.

*Permanent address: St. Olaf College, Northfield, Minn. 55057.

† Permanent address: University of Zaragoza, Zaragoza, Spain.

‡ Permanent address: Oklahoma State University, Stillwater, Okla. 74074.

¹J. E. Wertz, P. Auzins, R. A. Weeks, and R. H. Silsbee, *Phys. Rev.* **107**, 1535 (1957).

²J. E. Wertz, J. W. Orton, and P. Auzins, *Discuss. Faraday Soc.* **30**, 40 (1962); *J. Appl. Phys. (Suppl.)* **33**, 322 (1962).

³A. J. Tench and R. L. Nelson, *Proc. Phys. Soc. London* **92**, 1055 (1967).

⁴B. Henderson and A. C. Tomlinson, *J. Phys. Chem. Solids* **30**, 1801 (1969).

⁵J. W. Culvahouse, L. V. Holroyd, and J. L. Kolopus, *Phys. Rev. A* **140**, 1181 (1965).

⁶J. W. Carson, D. F. Holcomb, and H. Ruchardt, *J. Phys. Chem. Solids* **12**, 66 (1959).

⁷K. E. Mann, L. V. Holroyd, and D. L. Cowan, *Phys. Status Solidi* **33**, 391 (1969).

⁸W. P. Unruh and J. W. Culvahouse, *Phys. Rev.* **154**, 861 (1967).

⁹L. E. Halliburton, D. L. Cowan, and L. V. Holroyd, *Solid State Commun.* **12**, 393 (1973); *Phys. Rev. B* **12**, 3408 (1975).

¹⁰A. L. Allsop, J. Owen, and A. E. Hughes, *J. Phys. C*

6, L337 (1973).

¹¹M. M. Abraham, Y. Chen, W. C. Peters, J. Rubio O., and W. P. Unruh, *J. Chem. Phys.* **71**, 3658 (1979).

¹²L. S. Welch, A. E. Hughes, and G. P. Pells, *J. Phys. (Paris)* **7**, 198 (1976).

¹³A. E. Hughes and G. P. Pells, *J. Phys. C* **5**, 2543 (1972); **8**, 3703 (1975).

¹⁴P. Weightman and T. P. P. Hall, *J. Phys. C* **6**, 1292 (1973).

¹⁵J. F. Boas, T. P. P. Hall, and A. E. Hughes, *J. Phys. C* **6**, 1639 (1973).

¹⁶M. M. Abraham, W. P. Unruh, and Y. Chen, *Phys. Rev. B* **10**, 3540 (1974).

¹⁷F. A. Modine, Y. Chen, R. W. Majors, and T. M. Wilson, *Phys. Rev. B* **14**, 1739 (1976).

¹⁸J. Feldott, G. P. Summers, T. M. Wilson, H. T. Tohver, M. M. Abraham, Y. Chen, and R. F. Wood, *Solid State Commun.* **25**, 839 (1978).

¹⁹R. L. Miehler, *Phys. Rev. Lett.* **8**, 362 (1962).

²⁰B. S. Gourary and F. J. Adrian, *Phys. Rev.* **105**, 1180 (1957).

²¹A. E. Hughes and B. Henderson, in *Defects in Crystalline Solids I*, edited by J. H. Crawford, Jr., and L. M. Slifkin (Plenum, New York, 1972).

²²W. C. Holton and H. Blum, *Phys. Rev.* **125**, 89 (1962).

²³R. F. Wood, *Phys. Status Solidi* **42**, 849 (1970).

²⁴A. H. Harker, *J. Phys. C* **7**, 3224 (1974).